



LAWRENCE
LIVERMORE
NATIONAL
LABORATORY

LLNL-JRNL-401368

In-situ monitoring of surface post-processing in large aperture fused silica optics with Optical Coherence Tomography

G. M. Guss, I. I. Bass, R. P. Hackel, C. Mailhot,
S. G. Demos

February 14, 2008

Applied Optics

Disclaimer

This document was prepared as an account of work sponsored by an agency of the United States government. Neither the United States government nor Lawrence Livermore National Security, LLC, nor any of their employees makes any warranty, expressed or implied, or assumes any legal liability or responsibility for the accuracy, completeness, or usefulness of any information, apparatus, product, or process disclosed, or represents that its use would not infringe privately owned rights. Reference herein to any specific commercial product, process, or service by trade name, trademark, manufacturer, or otherwise does not necessarily constitute or imply its endorsement, recommendation, or favoring by the United States government or Lawrence Livermore National Security, LLC. The views and opinions of authors expressed herein do not necessarily state or reflect those of the United States government or Lawrence Livermore National Security, LLC, and shall not be used for advertising or product endorsement purposes.

In-situ monitoring of surface post-processing in large aperture fused silica optics with Optical Coherence Tomography

Gabe M. Guss, Isaac I. Bass, Richard P. Hackel, Christian Mailhiot, Stavros G. Demos
Lawrence Livermore National Laboratory
7000 East Avenue, Livermore, CA 94551, USA

Abstract

Optical Coherence Tomography is explored as a method to image laser-damage sites located on the surface of large aperture fused silica optics during post-processing via CO₂ laser ablation. The signal analysis for image acquisition was adapted to meet the sensitivity requirements for this application. A long-working distance geometry was employed to allow imaging through the opposite surface of the 5-cm thick optic. The experimental results demonstrate the potential of OCT for remote monitoring of transparent material processing applications.

OCIS codes: 170.4500, 120.4630, 140.3380

Laser systems that feature high power output are becoming increasingly important for manufacturing, military and basic science applications. Since a key limiting factor in the power output of laser systems most often remains the resistance of their optical components to laser induced damage, it is apparent that a new generation of materials or new methods to manufacture and post-process materials currently used in laser systems is needed. To increase the total output of the laser, large aperture designs have been employed which maintain the laser exposure fluence of the optical components below their damage threshold. For example, the fused silica lenses to be used to focus each of the 192 beams at 351 nm of the National Ignition Facility laser (Livermore, California, USA) onto a deuterium-tritium fusion target will be exposed to mean fluences as high as 8 J/cm² and local peak fluences of >14 J/cm². Surface damage over a 40 cm rectangular aperture of these fused silica components is known to initiate in this fluence range [1] which is about an order of magnitude below the intrinsic dielectric breakdown threshold of the pure bulk material. Damage initiation at these fluences arises from defects on the surface that cause coupling of laser energy into the material leading to formation of a crater with a network of cracks as well as the introduction of additional defects [2]. These material modifications cause additional damage upon subsequent exposure to laser pulses and the damage sites grow exponentially in diameter and depth [3].

Since there is no technology currently available to avoid laser induced damage, various post-processing techniques have been developed to mitigate the growth of damage sites, thus extending the lifetime and operability of high-value fused silica optics [4]. The most effective technique has been removal of the modified material within the region of the damage site by a combination of melting and ablation produced by a tightly focused 10.6 μm beam from a CO₂ laser. Damage sites as large as 300 μm in diameter with cracks 150 μm deep were successfully mitigated on small size (typically 5-cm in diameter, 1-cm thick) samples using fast-scanning galvanometers to move the 10.6 μm laser beam in a spiral pattern over the damage site [5]. Successful mitigation required removal of material to the deepest cracks. However, development of protocols to mitigate damage sites in large aperture optical components has been hindered by a lack of information about damage site morphology including subsurface cracks. The geometry of surface damage on large aperture lenses further complicates the problem of optical inspection.

If the inspection instrument is oriented to measure the subsurface cracks from the surface of the optic on which the damage is located, the probe light must penetrate through the fine grained silica rubble which forms the damage crater. In addition, the front surface may be occupied by the mitigation instrumentation (such as needed for CO₂ laser ablation or other method) further limiting the ability for in situ inspection. Therefore, imaging through the opposite surface of the optic might be the only feasible approach assuming it can be accomplished with adequate spatial resolution and working distance sufficient to cover the lenses thickness.

Optical Coherence Tomography (OCT) is an interferometric imaging technique that was initially developed to address various applications in the biomedical field [6]. It is particularly well suited for ophthalmic and tissue imaging applications that require millimeter depths of field with micrometer spatial resolution. Cross sectional imaging of laser damage using OCT through the front surface of the optic (the surface containing the damage site) has been previously reported [7]. The ability of OCT to detect subsurface cracks has also been demonstrated [7,8]. What makes OCT particularly interesting in the characterization of optical materials for large aperture laser systems is that its axial resolution can be maintained with working distances greater than 5 cm, whether viewing through air or through the bulk of thick optics. This allows imaging through the opposite surface of the optic. This unique combination of capabilities of OCT compared with other 3D profiling systems is explored in this work as a method to precisely measure the 3D spatial characteristics of laser induced surface damage sites through the opposite surface of fused silica large aperture optical components. An image processing approach was applied to achieve optimal detection of all features of interest such as the smallest cracks radiating from the bottom of the crater. The results demonstrate that OCT is a unique and valuable tool for in-situ characterization of damage sites and to guide and optimize mitigation on large aperture, high-value optics.

Our work was conducted by adapting to our application a commercial profilometer based on low coherence interferometry (μ Cam-3D fiber profilometer) designed by Novacam Technologies, Inc., (Pointe-Claire, Canada). The main components of the interferometer design are: a wide bandwidth super luminescent diode light source; a variable, high-speed optical path length scanning device (based on rhombic prisms scans allowing for collection of data at a rate of 300 axial scan-lines per second [9]); a fiber coupled measurement probe and a photodiode detector with associated electronic filtering; data acquisition and digital signal processing (DSP). Interference fringes occur when the optical path length of light traveling in the reference and sample legs of the interferometer are nearly the same. The axial resolution is determined by the width of the interference peak which was determined to be about 20 μ m. The lateral resolution of the instrument is determined by the diameter of the spot generated by the focus lens. This diameter varies from 25 to 30 μ m over a 4-mm axial region. A schematic of the experimental arrangement depicting the imaging geometry is shown in Figure 1.

Using this approach, we first evaluated the accuracy of the 3D OCT images of subsurface damage measured through the opposite surface at a working distance of 5 cm by comparing with conventional microscopy. This was accomplished by generating the damage on slab of fused silica polished on all sides thus allowing conventional microscopy from two orthogonal directions. Damage was generated by focusing a 355 nm wavelength pulse of light on the surface of the fused silica. The spot size was 75 μ m with a fluence which varied between 50 and 200 J/cm². This process creates damage which has varied amounts of subsurface cracking suitable for comparing OCT and microscopy.

An artifact inherent to the OCT system generate interference side-lobes with signal levels of the order of 1% of the peak interference (primary) signal at distances extending 100 μm from the location of registration of the peak. Side-lobes from bright features such as the undamaged surface of the optic or the bottom of the damage crater have the potential of masking the primary signal from weaker features of interest in our application such as subsurface cracks. To address this problem, a data analysis approach was developed to filter out the contribution of these side-lobes. Specifically, the side-lobe pattern of the OCT signal from a feature was calibrated using the signal generated by the polished surface of a fused silica sample. A set of calibration curves as a function of the peak amplitude was then obtained by tilting the sample to vary the signal amplitude. A simple algorithm was implemented in the data analysis to convert the signal from each vertical line in a cross-sectional image into a list of point locations. The algorithm begins by finding the location of the largest peak in the line. The x-y-z location of this peak is saved. The intensity of the peak is then used to select the appropriate calibration curve, which includes the main peak and side lobes. The calibration curve is registered to the peak in the line and subtracted from the data, thus reducing the signal from that feature below the background level of the line. This process is repeated for the next largest amplitude peak, iteratively until the remaining peaks are below a threshold value. This threshold level is determined by measuring the standard deviation of the background signal for each line in a region which is known to have no features. We empirically determined this threshold value to be about 10 times the measured standard deviation.

The side-view images coupled with top-view images gave information about the shape and morphology of both surface damage and subsurface cracks as shown in Fig. 2. The transverse area covered was a 2-mm square, and the axial distance of interest was 1-mm long extending from just above the surface to well below the damage site. The scans collected data at 5- μm step size in all three dimensions. The microscope images were collected with a standard 10x objective and scaled using a calibration reticule. The OCT data was rotated and plotted to match the viewing direction of the microscope as shown in Fig. 2. The color scale in Fig. 2c represents the depth with the surface (denoted as zero depth) shown in white color in order to separate out the image contribution of the damage site (in color) from that of the surface (white background).

The comparison between the standard longitudinal microscope image is visually comparable to the projection of the OCT data onto the xy-plane (see Figs. 2a and 2c). The deepest crack is 300 μm below the surface and is located at the same transverse position in both the microscope image and the OCT plot. The crack starting in the lower left of the top-view microscope image at (-200, -200) is seen from the OCT data to extend from the surface downward into the bulk toward the center of the damage. This type of cracks is known to be shallow. This is confirmed by the surface plane projection of the OCT image which reveal that this crack is located in the 0 to 50 μm depth region. In the same images, the radial crack extending in the (175, 200) direction is located at a depth of 200 μm as indicated by the OCT image. The depth of this crack is impossible to determine from the microscope image. The corresponding side-view images shown in Figs. 2b and 2d also highlight the ability of OCT to accurately image subsurface cracks. The crack which occurs at a depth of 250 μm and at a transverse location of 200 μm in the microscope image, is determined to be two cracks in the OCT image. This view from the conventional microscope is blurred due to one of the overlapping cracks being out of the microscopes focus plane. These examples demonstrate that the OCT image contains more information about the structure of the damage site compared to conventional microscopy which

is limited by inadequate interpretation of overlapping complex structures that may be in or out of focus during viewing.

Another major benefit of OCT over other inspection techniques is the long working distance which allows measurement of subsurface cracks not obtainable by any other known technique. The potential of this approach is best demonstrated in Fig. 3a and 3b where the images of damage sites located on the surface of a large size optic (40 x 40 cm² in lateral dimensions, approximately 5 cm thick) are shown as recorded by our OCT system. More specifically, this figure shows the superposition of the OCT image projection on the xz plane prior to (in red) and after (in green) mitigation. The image prior to mitigation allows the exact dimension of the damage site and its subsurface cracks to be evaluated and the correct parameters of the CO₂ laser ablation protocol to be determined. The image after mitigation shows that all the features of interest in the damage site including the cracks located below the crater have been removed. The OCT image of the mitigated site is more difficult to acquire due to limited reflection of the mitigated crater surfaces but there is enough reflection near the bottom that allows for accurate determination of the depth of the mitigated site.

The modified commercial instrument employed in this work is based on the so called “time domain detection” [6]. This design is limited in the maximum achievable acquisition speed by the mechanical optical delay element which, in our case, utilizes scanning rhombic prisms with a 90 percent duty factor that provides 300 axial line-scans per second. As a result, the total time to acquire the OCT data presented in this work is on the order of 1 minute per damage site. This image acquisition speed is not sufficient for in-line imaging during mitigation. However, the “Fourier domain” detection techniques that have recently been proposed improve the scanning speeds by employing either a spectrograph or a fast narrow band frequency swept laser source to spectrally encode the backscattered light from different depths. With these new methods, line rates acquisition rates of the order of 100 kilohertz have been demonstrated [10-12]. These new designs may allow for in-line imaging during mitigation at least to the degree that image processing time does not interfere with the display of the image in real time.

The application of OCT presented in this work to image defective regions of fused silica surfaces created by laser induced damage highlights its potential for use as a remote monitoring technique in materials processing applications. Although this potential has been recognized [13-15], the adaptation of OCT outside the biomedical research and diagnostics fields has been very limited. Typically, OCT imaging in tissues involves thin probes that can reach interior body locations through the vascular system, hand held devices in contact with the tissue for skin, oral or dental imaging and systems for examination of the eye. It is possible that because of its implementation in the biomedical field with instrumentation that requires contact or close proximity with the tissue, it has not been adequately appreciated that OCT images can be acquired at a large distance from the target object. In our case, this feature has enabled the high resolution imaging of the damage sites through the ≈ 5 cm thickness of a large aperture fused silica lens.

This work was performed in part under the auspices of the U.S. Department of Energy by Lawrence Livermore National Laboratory under Contract DE-AC52-07NA27344.

References

1. A. K. Burnham, L. A. Hackel, P. J. Wegner, T. G. Parham, L. W. Hrubesh, B. M. Penetrante, P. K. Whitman, S. G. Demos, J. A. Menapace, M. J. Runkel, M. J. Fluss, M. D. Feit, M. H. Key, and T. A. Biesiada, Proc. SPIE, **4679**, 173, 2002
2. S. G. Demos, M. Staggs, M. R. Kozlowski, Applied Optics, **41**, 3628, 2002
3. M. A. Norton, L. W. Hrubesh, Z. Wu, E. E. Donohue, M. D. Feit, M. R. Kozlowski, D. Milam, K. P. Neeb, W. A. Molander, A. M. Rubenchik, W. D. Sell, P. J. Wegner, Proc. SPIE, **4347**, 468, 2001
4. L. W. Hrubesh, M. A. Norton, W. A. Molander, E. E. Donohue, S. M. Maricle, B. Penetrante, R. M. Brusasco, W. Grundler, J. A. Butler, J. Carr, R. Hill, L. J. Summers, M. D. Feit, A. M. Rubenchik, M. H. Key, P. J. Wegner, A. K. Burnham, L. A. Hackel, and M. R. Kozlowski, Proc. SPIE, **4679**, 23, 2002
5. I. L. Bass, G. M. Guss, and R. P. Hackel, Proc. SPIE, **5991**, 59910C, 2005
6. D. Huang, E.A. Swanson, C.P. Lin, J.S. Schuman, W.G. Stinson, W. Chang, M.R. Hee, T. Flotte, K. Gregory, C.A. Puliafito, and J.G. Fujimoto, Science, **254**, 1178-1181 (1991).
7. S. G. Demos, M. Staggs, K. Minoshima, and J. Fujimoto, Optics Express, **10**, 25, 2002
8. M. Bashkansky, D. Lewis, V. Pujari, J. Reintjes, H. Y. Yu., NDT&E International, **34**, 547, 2001
9. M. L. Dufour, G. Lamouche, S. Vergnole, B. Gauthier, C. Padioleau, M. Hewko, S. Levesque, and V. Bartulovic, Proc. SPIE, **6343**, 63431Z, 2006
10. N.A. Nassif, B. Cense, B.H. Park, M.C. Pierce, S.H. Yun, B.E. Bouma, G.J. Tearney, T.C. Chen, and J.F. de Boer, Opt. Express **12**, 367, 2004.
11. R. Huber, M. Wojtkowski, K. Taira, J.G. Fujimoto, and K. Hsu, Opt. Express **13**, 3513, 2005.
12. Y. Yasuno, V. Madjarova, S. Makita, M. Akiba, A. Morosawa, C. Chong, T. Sakai, K. Chan, M. Itoh, and T. Yatagai, Opt. Express **13**, 10652, 2005.
13. C. W. Xi, D. L. Marks, D. S. Parikh, L. Raskin, S. A. Boppart, Proceedings of the National Academy of Sciences of the United States of America, **101**, 7516, 2004
14. P. Targowski, B. Rouba, M. Wojtkowski, A. Kowalczyk, Studies in Conservation, **49**, 107, 2004
15. D Stifter, Applied Physics B-Lasers and Optics, **88**, 337, 2007

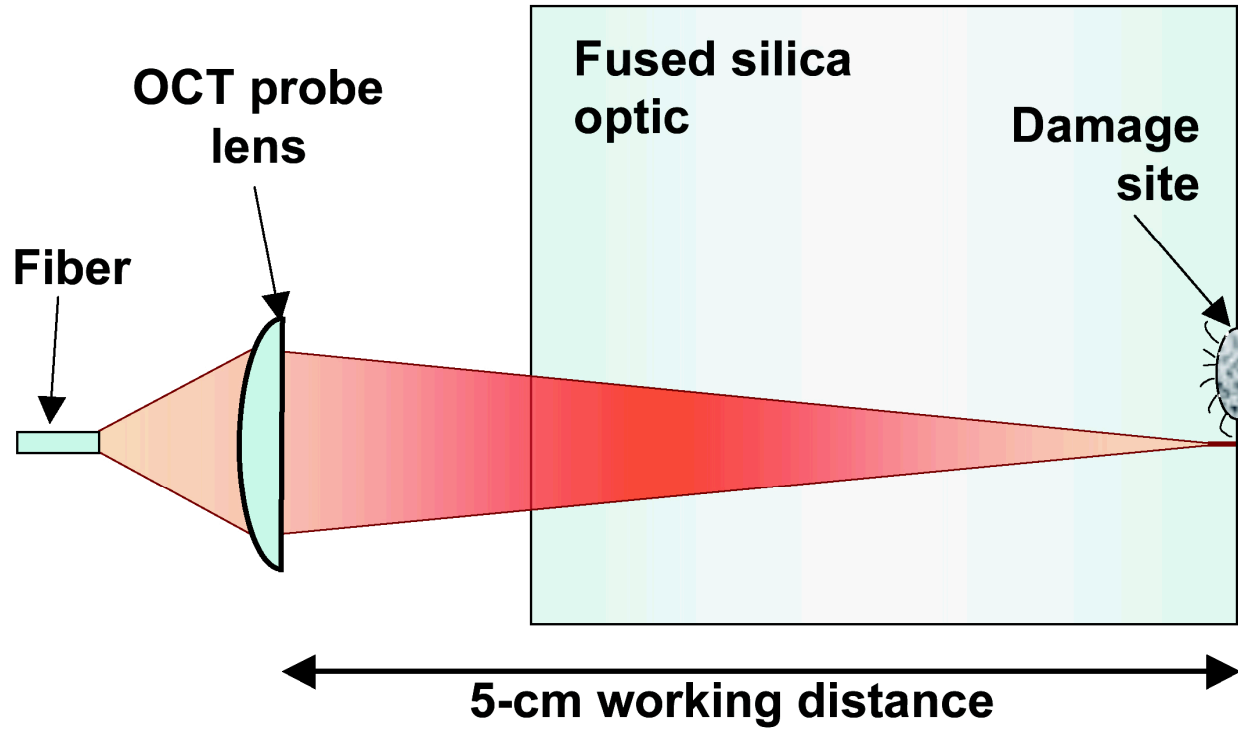


Figure 1: Schematic depicting the experimental arrangement for OCT imaging of surface damage sites through the opposite surface of a large aperture fused silica optic

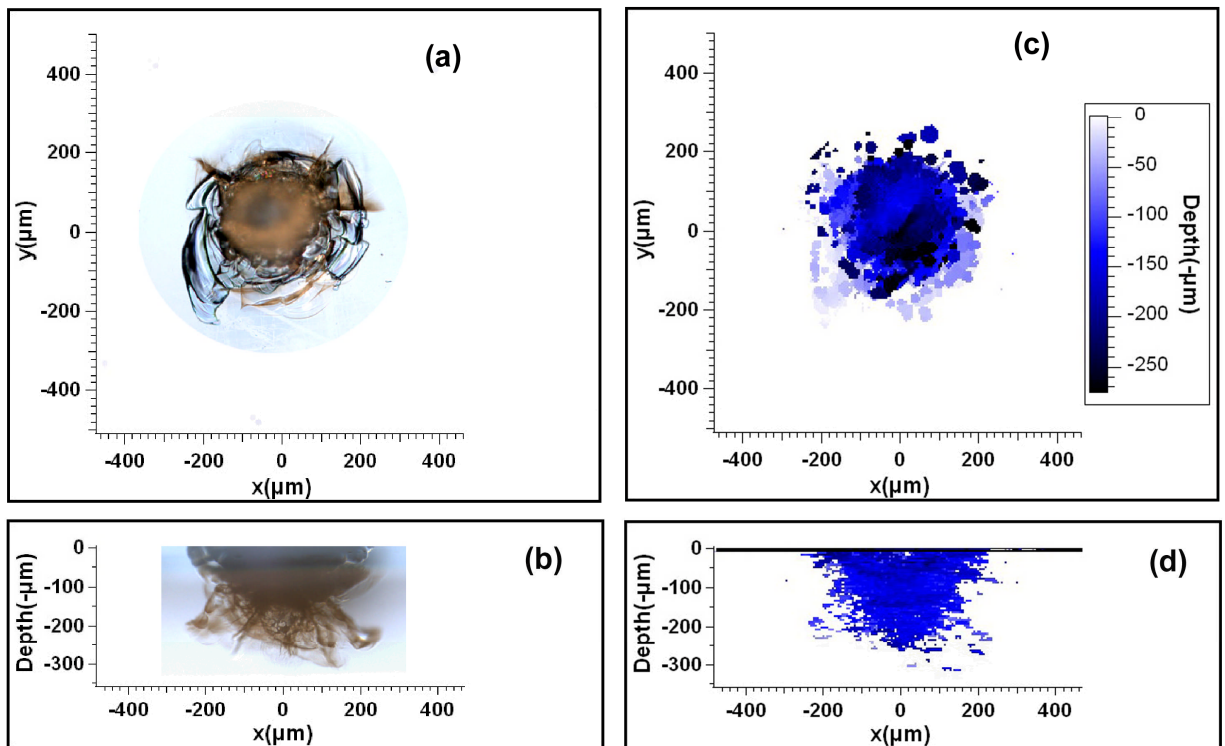


Figure 2: Images of the same surface damage site. a) Top view and b) side view conventional microscope images. Projections of the 3-D OCT image on c) the surface plane and d) the axial plane that correspond to the viewing orientation of the conventional images

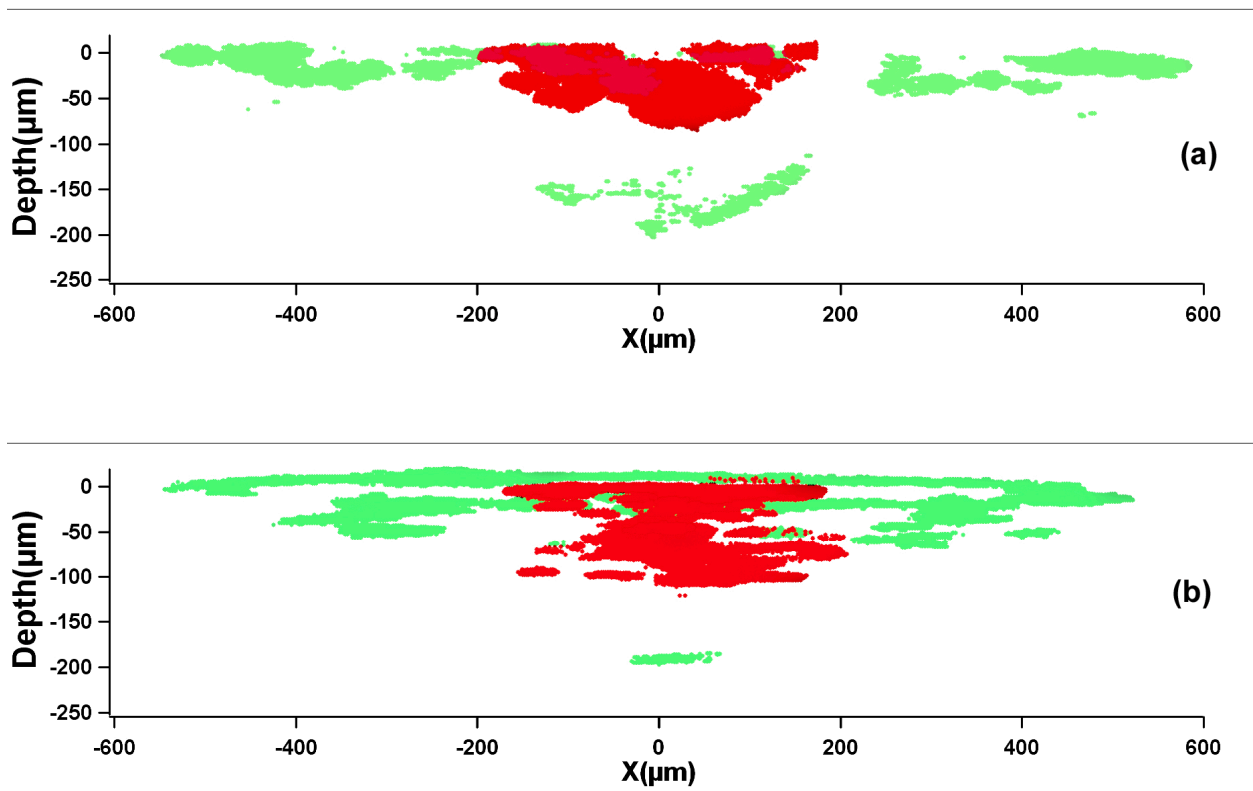


Figure 3: Superimposed projections of OCT images of two different damage sites located on the surface of a large aperture fused silica optics taken before (in red color) and after CO_2 laser mitigation (in green color).